CRUISE REPORT

Alaska **L**angseth **E**xperiment to **U**nderstand the mega**T**hrust (ALEUT) project

Leg 1 – OBS acquisition:

Kodiak – Sand Point

29 June – 11 July 2011

Leg 2 – MCS acquisition

Sand Point – Dutch Harbor

11 July 2011 – 5 August 2011

Table of Contents

Appendices:

1. Cruise Objectives

The aim of this program is to characterize the megathrust, overriding and downgoing plates, and other fault systems associated with the Alaska-Aleutian subduction zone from the Shumagin gap, across the Semidi segment, to the western end of the Kodiak asperity. To achieve this, we will use multichannel seismic (MCS) reflection and wide-angle reflection/refraction (WARR) data, and relate the reflection and velocity images to the mechanical behavior of the megathrust and other faults based on the history of subduction earthquakes [Davies et al., 1981], historical intraslab and crustal earthquake hypocenter distribution, present-day locking of the plate boundary from GPS data [Fournier and Freymueller, 2007], and other available constraints. A secondary goal of the cruise is to conduct an oceanographic experiment to study the mixing processes in this area by acquiring hydrographic (XBT/XSV/XCTD/sea-surface salinity) data that are coincident in space and time with the collected MCS data. In support of the science objectives, we will collect the following coincident supplementary data: multibeam, sea bottom profiler (3.5 kHz Knudsen), magnetic, gravity, and navigation.

Downdip limit of the seismogenic zone

The largest and most destructive earthquakes, with magnitudes greater than 8-9, occur on subduction zone megathrusts. A great source of uncertainty in probabilistic seismic hazard maps for such earthquakes is the downdip limit of the seismogenic part of the megathrust. Competing models assert that the downdip limit is controlled by temperature (e.g., 300-450ºC; Scholz, 1998) or by the intersection of the plate boundary with the forearc mantle, which might be weak due to serpentinization [Tichealaar and Ruff, 1993; Peacock and Hyndman, 1999, Oleskevich et al., 1999](Fig. 1.1). Downdip of the locked zone, the megathrust transitions from stick-slip behavior to stable sliding. In some subduction zones, slow slip events and tremor are associated with this downdip transition [e.g., Dragert et al., 2001; Rogers and Dragert, 2003].

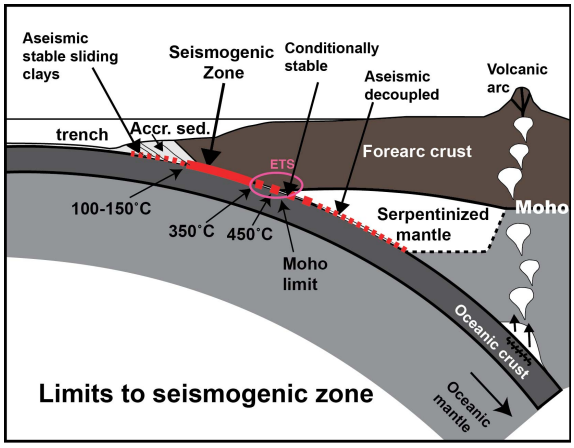

***Figure 1.1**: Illustration of possible controls on the plate boundary modified after Oleskevich et al., 1999*

Independent constraints are needed on the extent of the locked zone and the variations in properties at the plate boundary downdip from the locked to transition zone. A study of the northern Cascadia subduction interface revealed an intriguing spatial correlation between the seismic reflection character of the megathrust and its mechanical behavior [Nedimović et al., 2003]. In the seismogenic, locked portion of the megathrust, which is located primarily offshore, the thrust is characterized by a single reflection event or a very thin reflection package. In the transition zone downdip of the locked zone, the megathrust reflection package thickens dramatically and exhibits a more complex signature (Fig. 1.2). Nedimović et al. [2003] proposed that this distinctive reflection signature might make it possible to directly image and map the location of the locked/transition zone boundary. Deep reflection images from Alaska [Fisher *et al.*, 1989; Moore *et al.*, 1991], Chile [Groß *et al.*, 2008] and SW Japan [Kodaira *et al.*, 2002; Kodaira *et al.*, 2004] show a megathrust signature much like the one observed at northern Cascadia, suggesting

that reflectivity patterns similar to those in Cascadia are widespread.

The eastern Alaska-Aleutian subduction zone is an ideal place to examine the downdip edge of the seismogenic zone and assess its characteristics in active-source seismic data for several reasons. It is one of the few places where the locked/transition zone boundary lies completely offshore and is fully accessible to marine profiling. The downdip limit of coseismic slip in our study area is known from large subduction zone earthquakes in 1938 and 1964. During the 20th century, virtually the entire Alaska-Aleutian subduction interface has ruptured in large to great earthquakes with rupture areas, seismic moments, and magnitudes of several of these shocks among the largest known anywhere in the world [Davies *et al*., 1981]. The 1938 rupture area and surrounding regions on which we are focusing also broke in 1788 and 1847, and may have broken between 1899 and 1903 [Sykes *et al*., 1971]. This region is of great topical interest because 73 years have passed since the 1938 earthquake, and average megathrust repeat times for this zone appear to be 50 to 75 years. The seismic reflection results can also be compared to estimates of the downdip limit that are based on geodetic post-seismic uplift data [Fournier *et al*., 2007] and thermal modeling (e.g., Hyndman and Wang, 1993, 1995).

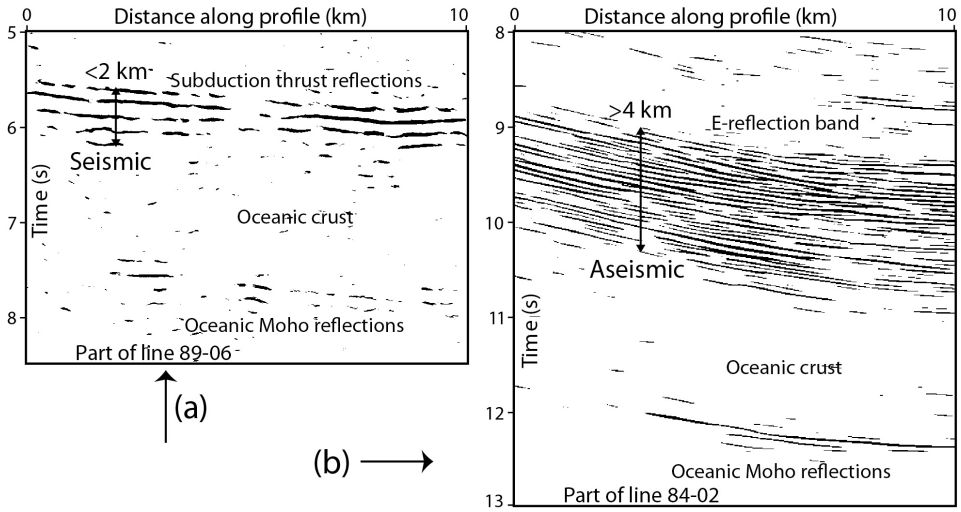

Figure 1.2*: Two details from MCS data from the Cascadia subduction zone showing (a) Thin (<2 km) reflection package from the interpreted locked portion of the thrust, and (b) Thick (>4 km wide) band of reflections overlying the subducted oceanic crust in an area where aseismic (stable) slip regime has been observed (Nedimović et al., 2003).*

Ongoing work suggests that tremor and slow slip are common at the downdip edge of the Alaska/Aleutian subduction zone [Petersen and Christensen, 2009; Brown *et al*., 2010]. Our new dataset will provide key constraints on the depth, nature and geometry of the megathrust, which can be integrated with information on ETS events as they become available in order to better constrain the origin of these events and the processes that are responsible for them.

Along-strike variations in locking

Coupling and slip behavior vary substantially at subduction zones around the world. This variability in megathrust behavior has been attributed to many factors such as the speed and direction of plate convergence, stress state in the overriding plate, age and thermal structure, the abundance and nature of sediment entering the trench, and to seamounts or other heterogeneities on the overriding or downgoing plate (e.g., Ruff and Kanamori, 1980, 1983; Uyeda and Kanamori, 1979; Cloos, 1992; Hyndman and Wang, 1995, Kodaira et al., 2004), although it is possible that the incompleteness of the historic record leads to much of the variability (McCaffrey, 1997, 2007). It is difficult to untangle possible controlling factors by comparing

different subduction systems because too many parameters vary between them.

The Alaska/Aleutian subduction zone offers a unique window into controls on locking and seismogenesis because large changes in locking appear to occur over relatively short distances within this individual system. The coupling between the Pacific and North America plates varies from no or weak coupling in the Shumagin gap to strong or full coupling for the northeastern part of the 1938 earthquake rupture area and southwestern part of the 1964 earthquake rupture area [Freymueller and Beavan, 1999; Zweck *et al*., 2002; Fournier *et al*., 2007](Fig. 1.3). By surveying across the variably coupled parts of the megathrust, we hope to determine what aspects of the subduction zone vary along strike, such as roughness and hydration of the downgoing plate, incoming and subducted sediment thickness, and structure of the overriding plate. We also hope to establish if lateral variations in coupling are observable in the megathrust reflection signature. Establishing a link between slip behavior and attributes in seismic reflection data is important because it can provide information on the dominant type of deformation for the areas of the megathrust that have slipped seismically during subduction earthquakes but presently appear to be weakly coupled because of long recurrence intervals [McCaffrey, 2007].

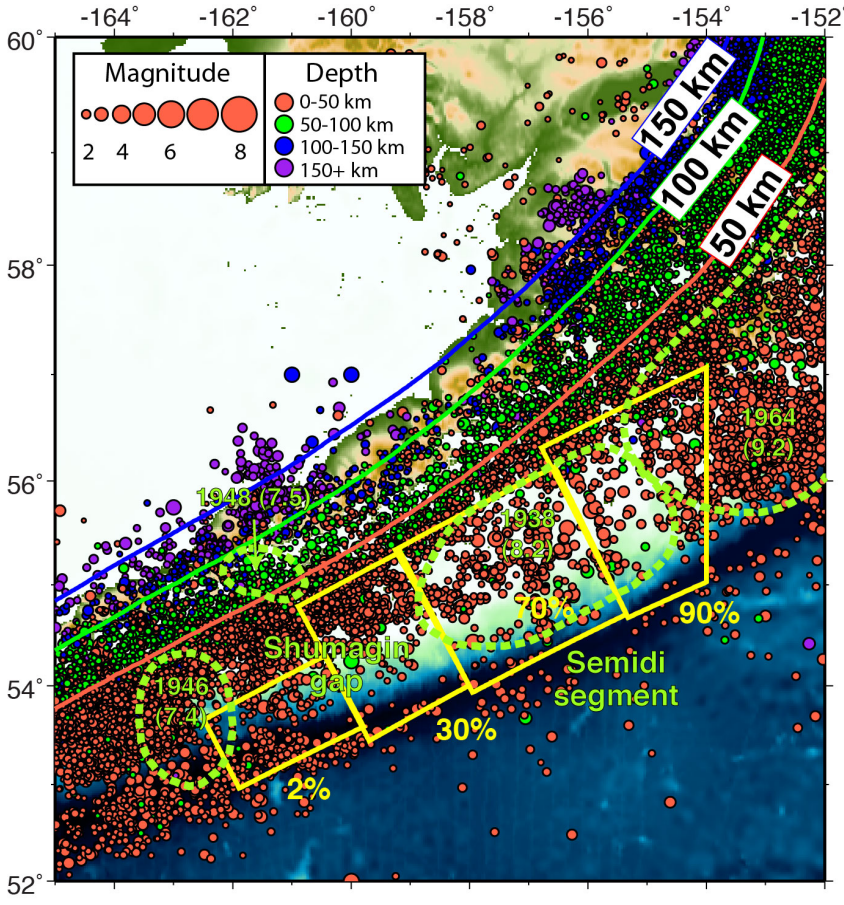

Figure 1.3*: Map of seismicity from the AEIC catalogue colored by depth and sized by magnitude. Yellow polygons and numbers denote modeled coupling from geodetic data (Fournier and Freymueller, 2007). Green dashed lines are estimated rupture zones from Davies et al. 1981. Note the apparently greater abundance of events in the creeping Shumagin gap than in the locked Semidi segment.*

Hydration of downgoing plate

Water stored in pore space and as hydrous minerals in the sediments, crust and upper mantle of the subducting plate is later released landward of the trench through dewatering and dehydration processes. The volume of water brought into the subduction zone, the distribution of water in the sediments, crust and upper mantle, and the depths at which it is released have a profound impact on a wide variety of magmatic and deformational processes in subduction zones. The amount of water and thermal structure of the subduction zone control when and how much water is released in the forearc versus the arc, which may effect the availability of water beneath arcs and thus their magmatic productivity

[Wada and Wang, 2009]. The volume of water exerts a strong control on the crystallization sequence of arc magmas [Müntener *et al*., 2001]. The presence of water also strongly affects the physical properties of rocks and can significantly reduce the temperature at which the transition from brittle to ductile deformation occurs (e.g., Scholz, 2002), which may be responsible for the changes in the megathrust slip nature at the downdip limit of the seismogenic zone. The introduction of fluids can lead to the development of pore fluid overpressures at the plate interface (Kodaira et al., 2004) and/or within the downgoing plate [Audet *et al*., 2009], which strongly influence the mode of deformation. At greater depths, dehydration embrittlement is the most plausible earthquake mechanism for intraslab events at intermediate depths of 50-300 km (e.g., Green and Houston, 1995; Peacock, 2001).

Hydration of oceanic lithosphere begins near the ridge axis due to faulting and hydrothermal circulation, but is mostly constrained to the top several kilometers of the oceanic lithosphere due to high temperatures. Significant additional hydration occurs as the plate bends at the trench axis (Fig. 1.4). Seawater can percolate into the crust and mantle along normal faults formed in the downgoing plate during bending [Ranero et al., 2003]. The degree of hydration that occurs during bending is controlled by a range of parameters, including the age and temperature regime of the downgoing plate, the thickness of sediments, and the amount and style of bending related deformation (e.g., Nedimović et al., 2009). The ease with which pre-existing faults in the oceanic crust can be reactivated, such as inherited trench-parallel fabric, may be important for controlling the extent of mantle serpentinization.

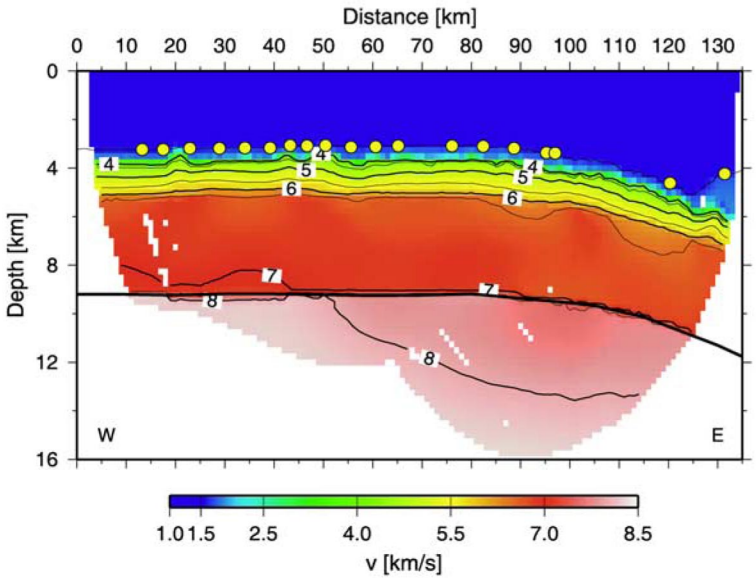

Figure 1.4*: Velocity model of the downgoing plate in the Central American subduction zone showing reduced velocities in the mantle associated with plate bending, interpreted to arise from serpentinization (Ivandic et al., 2008)*

The Alaska/Aleutian subduction system provides a useful comparison to well-studied hydration in the Central American slab because anticipated oceanic fabrics are expected to be both nearly orthogonal to the trench in some areas and parallel to the trench in other areas based on spreading directions inferred from magnetic anomalies. Intermediate-depth seismicity is well documented in the area of our study (e.g., Abers, 1992). Intriguingly, the Semidi segment is characterized by much lower historical intraslab seismicity rate than the Shumagin gap and Kodiak asperity www.giseis.alaska.edu/Seis/html_docs/regional_seismicity.html). Relating the change in depth and extent of oceanic plate hydration at the outer trench wall, to the change in density and distribution of intraslab events may provide insight into the maximum magnitude for these events. We can also compare any along strike variations in hydration and bending with variations in rupture history and present-day coupling of the megathrust (Fournier and Freymuller, 2007).

Seismic Oceanography

Seismic Oceanography (SO) is a recent discipline that is based on using the MCS data, traditionally collected for geological prospection to image the oceanic water column. Oceans have inner coherence structures of salt and temperature contrasts such as fronts, currents, and eddies generated by mixing processes that determine the energy and material transport. In SO, the reflections recorded in the MCS data result from sound speed and density changes in the water column that are caused by variations in temperature and salinity. The MCS data and imaging technique provide the potential of realizing long sections of near-synoptic 2D and swath 3D images of ocean fine structure (Mirshak et al., 2010). With this method, the internal water column structure is imaged with a resolution on the order of 10 m, both horizontally and vertically, which is ~100 times higher horizontal resolution than the one provided by classical oceanographic instrumentation (Holbrook et al., 2003). The high horizontal resolution and synopticity of SO data provide new information about the lateral coherence and horizontal characteristics of the fine structure and its interaction with mesoscale structures that are analyzed in order to better understand the mixing processes involved.

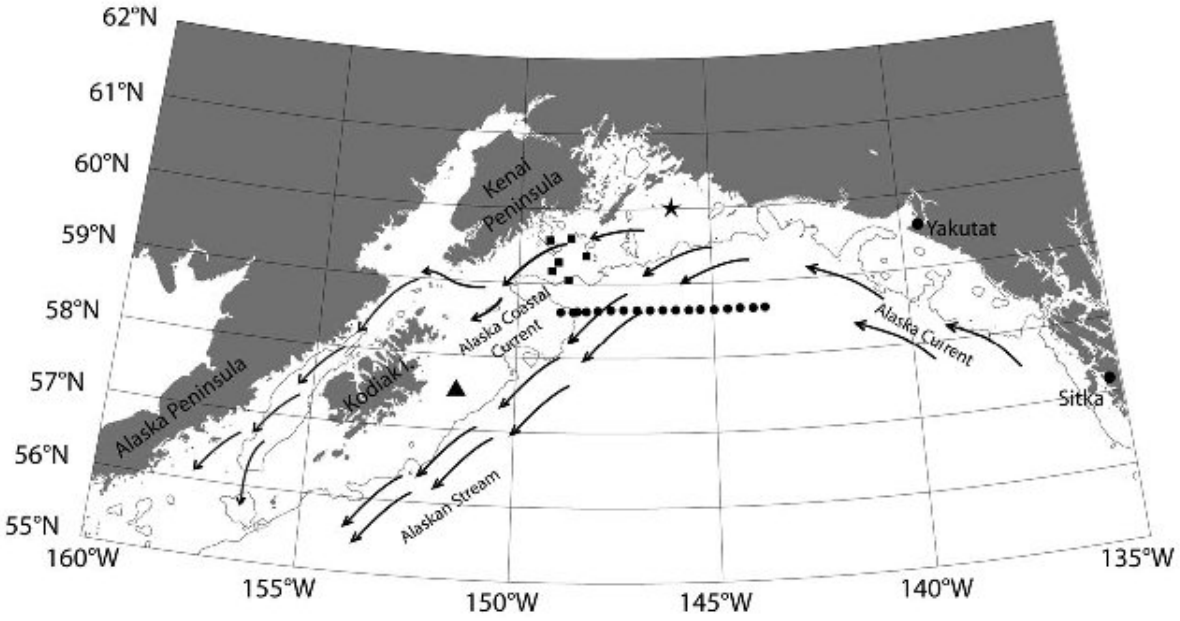

Figure 1.5*: Map of the Alaska Stream and Alaska Coastal Current (Ladd et al 2005).*

Circulation in the Gulf of Alaska (GOA) is dominated by two current systems, the cyclonic subartic gyre in the basin and the Alaska Coastal Current (ACC) on the continental shelf. At the head of the GOA, the ACC turns southwestward following the shelf-break and forms the Alaska Stream (Fig. 1.5). The GOA supports a rich ecosystem, including numerous species of fish, marine mammals and seabirds. The significant amount of nutrients in the GOA is supplied by strong mechanisms of cross-shelf exchange and mixing, which include episodic upwelling, eddies and tidal mixing combined with bathymetric steering (Ladd et al, 2005, Cummis et al, 2001). The priority of this SO experiment is to image the fine structure generated by these mixing processes along the shelf-break and upper slope. Particularly strong internal tides

radiating into the North Pacific are produced near the Amutka Pass, which is located along the Aleutian islands (Cummins et al., 2001) but west from our study area. Nevertheless, strong internal tides, or gravity waves propagating at tidal frequencies, especially the semidiurnal (M2) internal tides, are still present in our study area and will be the focus of our SO add-on experiment. The seismic data and corresponding reflection images of the water column will be compared with coincident and simultaneously recorded temperature, sound speed and salinity profiles acquired with XBT, XSV and XCTD probes.

2. Survey Plan

Our original survey plan consisted of five ~350-km-long MCS dip profiles and two OBS profiles coincident with two of the MCS profiles. The MCS profiles were designed to image the reflection and/or velocity structure of greatest importance for understanding and constraining the seismic hazards in the study area: the entire locked zone on the megathrust, as indicated by GPS data and estimated rupture zones of past earthquakes (Davies et al., 1981; Fournier and Freymuller, 2007). They also encompass the updip and downdip transitions to stable sliding, structures in the overriding plate such as splay faults and forearc basins, and structures in the downgoing plate such as bending related normal faulting and associated hydration of the oceanic crust and mantle. We extended the profiles as close as possible to the coast to image as far downdip as possible. At the south end, we also extended the profiles at least 80 km onto the downgoing oceanic plate to image deformation and hydration associated with plate bending [Ranero *et al*., 2003; Ivandic *et al*., 2008].

We planned to acquire the data with the full 6600 cu. in. source of the *Langseth* and two 8-km streamers. The source and one of the streamers would be towed at a depth of 12 m to maximize low frequencies (and deep imaging) while the second streamer would be towed at 9 m for better imaging the sediments and upper crust. Using long streamers would enable deeper and better reflection imaging and velocity constraints. In addition to expanding our range of frequencies and improving the signal-to-noise ratio, employing two streamers would allow for more sophisticated processing (e.g., swath processing (Nedimović et al., 2003) as well as very high precision streamer navigation using the acoustic network.

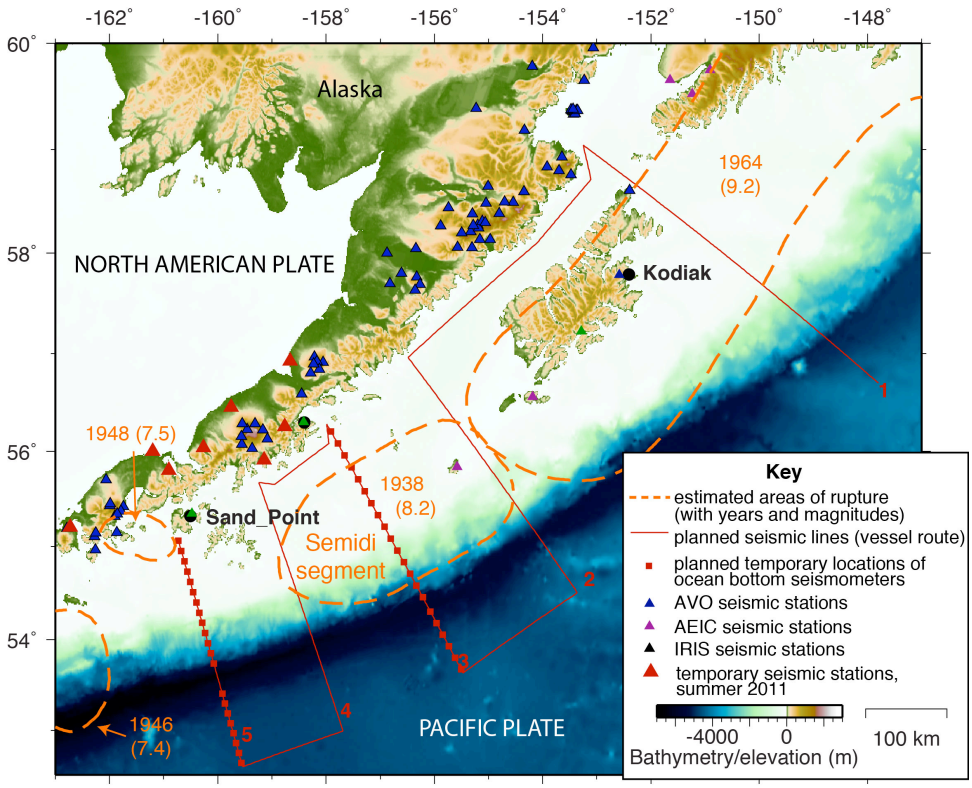

***Figure 2.1**: Map of planned survey*

The most easterly profile (Line 1 in Fig. 2.1) lies east of Kodiak and crosses part of the 1964 M9.2 rupture zone. This line is in the region of the existing EDGE profile [Moore *et al*., 1991], between the two highly-locked asperities of the subduction zone based on GPS data [Zweck *et al*., 2002]. We positioned this line here when we learned that we

could not shoot a profile immediately west of Kodiak through Sitkinak Strait, which passes through a locked zone, because of the shallow seafloor. Three of the planned profiles focus on the Semidi segment, which last ruptured in a M8.2 earthquake in 1938. One profiles is located in the center of the segment and two are near the edges (Lines 2-4 on Fig. 2.1). Finally, the fifth profile is positioned in the Shumagin gap, which has not had a historic great earthquake (Davies et al., 1981) and is thought to be freely slipping based on GPS data (Fournier and Freymuller, 2007). All of the lines were adjusted in coordination with the Marine Office to avoid overly shallow water depths and sensitive seal lion rookeries.

We planned to acquire the wide-angle seismic reflection/refraction data along two of the MCS profiles: Lines 3 and 5. These data should enable us to constrain deep crustal structure along the profile in the center of the Semidi segment and in the Shumagin gap. In particular, these data could constrain the deep geometry of the overriding and downgoing plates, hydration of the downgoing plate, wide-angle reflectivity of the megathrust, as well as provide us with velocities needed to depth migrate the deeper sections of the reflection profiles. We planned to place short-period, 4-channel ocean bottom seismometers spaced at ~13-16 km along these profiles and shoot to them with the full 6600 cu in source towed at 12 m to maximize low frequencies with long shot intervals (120 s, 310 m) to prevent previous shot noise.

3. Cruise Summary

MGL1110 achieved all of the core data acquisition objectives and was a complete success. As planned, we divided the cruise into two parts. During the first part (June 29 – July 12), we scouted selected portions of the planned MCS program and acquired OBS data. Wide-angle reflection/refraction data were acquired using the full 6600 cu. in. airgun array towed at 12 m and short-period 4-component Scripps OBS spaced at ~13-16 km along two ~400-km-long profiles coincident with MCS profiles across the Shumagin Gap (OBS Line 5) and Semidi segment (OBS Line 3)(Fig. 3.1). During the second part (July 12 – August 5), we acquired MCS data along ~3700 line-km, which included six dip lines (two in Shumagin Gap, three across the Semidi segment, and one over the Kodiak asperity within the 1964 rupture patch), a strike line that crossed from the locked Semidi segment to the freely slipping Shumagin gap, and a series of grid lines primarily targeting the structure of the downgoing oceanic plate. This was much more data than we expected to acquire (~2000 km). Most of the MCS data were acquired with two 8-km-long streamers and the full 6600 cu in source. The source and one streamer were towed at 12 m, while the second streamer was towed at 9 m. Problems with telemetry and the lead-in on the starboard streamer ultimately rendered it inoperable, so a portion of the MCS program was acquired with only one streamer (at 12 m). More details on both parts of the cruise are below.

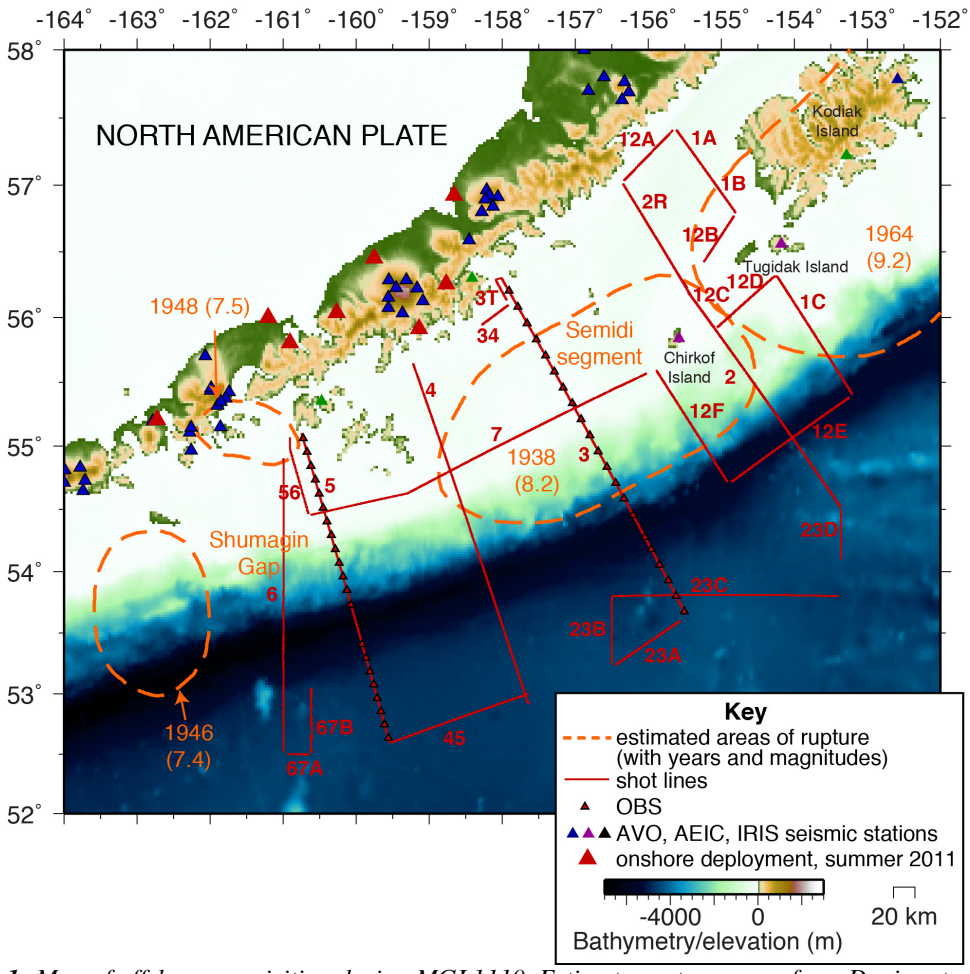

Figure 3.1: *Map of offshore acquisition during MGL1110. Estimate rupture areas from Davies et al. (1981).*

Scouting

During the first ~1.5 days of the cruise, we scouted the following parts of our planned MCS program (Fig. 2.1): 1) northern end of planned MCS line 1 and Shelikof Strait, where we were concerned about strong currents, fresh water from glacial runoff and marine mammals, 2) the northern end of Line 2, where we were concerned about shallow water depths, and 3) a shallow basement ridge on Line 2 between Tugidak and Chirkof islands. As we anticipated, we observed a large number of whales and low salinity water at northern end of Line 1 and in Shelikof Strait. Exposed rocks and shallow water were also observed at the northern end of Line 2. The basement ridge on the center of the shelf along Line 2 reached a minimum depth of 35 m, which was considered passable. The information gleaned during scouting strongly influenced our ultimate MCS shooting plan. We moved the northern end of Line 2 slightly to the east by adding a gentle dog-leg north of the basement ridge in the middle of the shelf (between Tugidak and Chirnof islands). After the MCS program was underway, we decided not to shoot Shelikof Strait and Line 1 because of the likely difficulty of acquiring data due to mammals and the long trip to get to this line.

OBS data acquisition

Following scouting, we began the OBS program on July 1. We deployed 21 OBS along Line 3 spaced at ~15.8 km. There is a slightly larger gap between OBS 306 and 307 to avoid deploying OBS in water depths greater than 5500 m (maximum depth allowed by the glass spheres of the Scripps instruments). We placed OBS as close as possible to the 5500-m isobath using centerbeam bathymetry values from the *Langseth*. We then shot the line away from the coast with the full 6600 cu in source towed at 12 m and a shot spacing of 310 m (~120 s). Two marine mammal powerdowns occurred near both ends of the line (between OBS 321 and 320, and between OBS 301 and 302). All 21 OBS were recovered in 43 hours (finishing on July 7); faster rise times were observed than expected (~48 m/min).

We then proceeded to Line 5, and deployed 21 OBS at a spacing of ~12.75 km. A larger gap (~40 km) was required over the deeper trench on this line to avoid water depths greater than 5500 m. Again, we placed the OBS as close as possible to 5500 m on either side of the trench. We shot the line away from the coastline using the same parameters as Line 3. A marine mammal powerdown occurred near OBS 521. All 21 OBS were recovered in 40 hours (again with relatively quick rise times). Following the completion of recoveries on July 12, the *Langseth* steamed into Popof Strait for a boat transfer at Sand Point. The Scripps OBS team and a mammal observer disembarked, and we were joined by eight new science party members, including 5 undergraduate students from Columbia, a postdoc from Dalhousie (Berta Biescas), and two science technicians.

MCS acquisition

Following the boat transfer, we began deploying the two 8-km streamers. This process ultimately required 73 hours. Many sections and modules needed be replaced, and parts of the streamers needed to be retrimmed during deployment. The failure of the slip ring on reel 1 and the lead-in on streamer 3 added considerable time to deployment. Following full deployment of the streamers and the 6600 cu in airgun array (76 hours after we began deployment), problems occurred with acquisition system (communication issues between navigation and acquisition systems), which required 7 hours to troubleshoot. Acquisition finally began in earnest near the end of the day on July 15.

We acquired MCS data on the four major dip lines west of Kodiak (MGL1110MCS02-05) as planned working from west to east. Only minor modifications were made to this portion of the survey plan. A grid of profiles orthogonal and parallel to the spreading direction of downgoing oceanic crust was shot between Lines MGL1110MCS02 and 03 in place of the planned, obliquely oriented connecting profile. We decided not to shoot our originally planned profile east of Kodiak due to the long round-trip transit and the poor likelihood of acquiring data on the landward portion of the line due to abundant marine mammals. Instead, we were able to acquire a two-part profile just east of Kodiak Island within the Kodiak asperity (and the western edge of the 1964 rupture), a strike line extending from the locked Semidi segment to the freely slipping Shumagin gap on the shelf and a westerly dip line within the freely slipping Shumagin gap. Revisions to our cruise plan were strongly limited by the bounds of our Incidental Harassment Authorization (IHA), which did not allow us to go west of 161ºW or south of 52.5ºN. The Marine Office strongly advised us not to seek permission to expand our box from the IHA because it would require a reassessment of all our revised profiles and could lead to the IHA being taken away and an early end to our program.

Occasional powerdowns (and rare shutdowns) were required throughout the MCS program for marine mammals. We only opted to reshoot two key portions: the landward end of Line 5 and a section of Line 2 near the estimated downdip end of the locked zone. Marine mammals were most commonly observed at the northern (landward) edges of the lines and west of Kodiak. However, on the whole, we experienced less downtime from marine mammals than anticipated.

We continued to have some difficulties with the streamers intermittently throughout acquisition. The starboard streamer began to have telemetry issues and stopped recording towards the end of profile MGL1110MCS04. Troubleshooting was undertaken during MGL1110MCS34. Both the slip ring and lead-in appeared to have problems. The slip ring was replaced, and the lead-in was diagnosed to be near its demise. By towing the starboard streamer off the stern (instead of off the paravane), it was possible to power it up, so we towed in tDhis configuration for the rest of the cruise. The starboard streamer ultimately stopped working near the beginning of MGL1110MCS12F, and we acquired data for the rest of the survey on the deeper port streamer. However, we could still use acoustic net to provide more accurate navigation for the single port streamer than would have been possible otherwise.

Densely spaced XBT and XSV deployments were conducted on the continental slopes of the major dip lines (Fig 3.2). On MGL1110MCS03-05, XBT's, XSV's and XCTD's were deployed at water depths from 300 to ~5000 m, but on profiles MGL1110MCS01A/B, 02 and 06, they were focused on upper part of slope above water depths of ~2000 m, where there appeared to be more fine-scaled structure. During the first couple of lines, nearly all the wires on the oceanographic probes broke, but greater success rates were achieved on later lines. The paravanes, height of the PVC pipe above the water and the wind had a large impact on likelihood of breaking wires (see appendix G for more details).

The quality of both the OBS and MCS data acquired during MGL1110 is exceptionally high. We undertook a range of onboard processing activities (see Section 6), which allowed us to evaluate the data. As described in Section 7, these data contain clear arrivals throughout the sediments, crust and upper mantle and will certainly enable us to address our scientific questions.

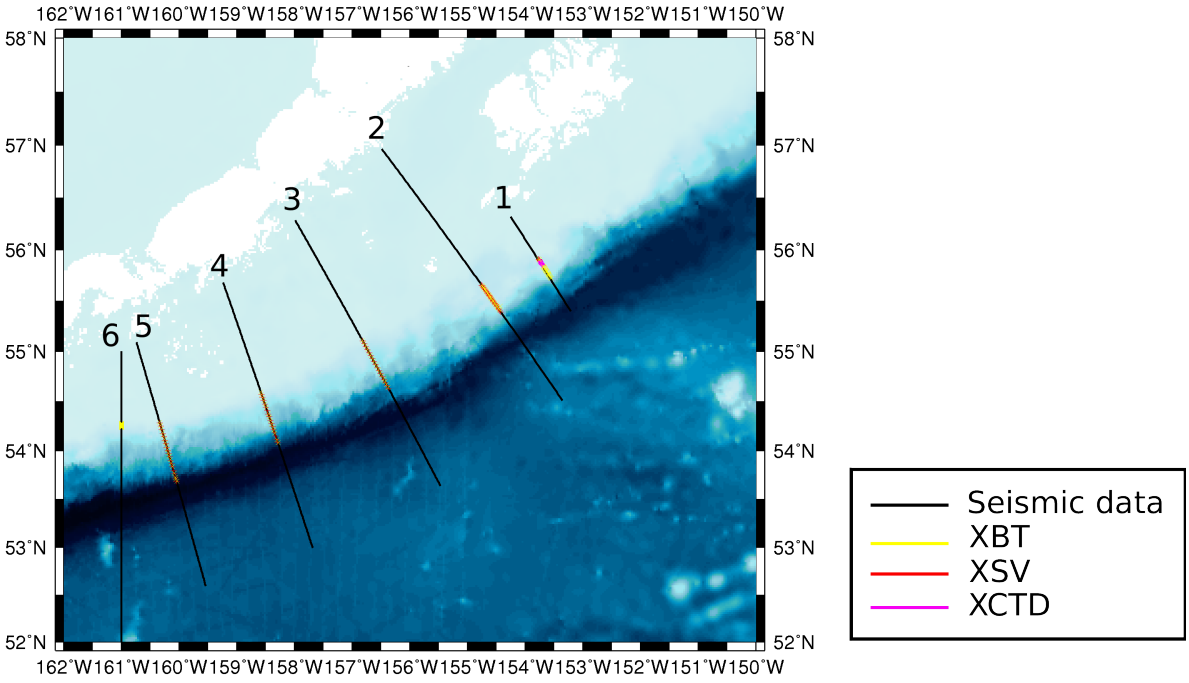

***Figure 3.2**: Location of the seismic lines and the oceanographic probes that were simultaneously acquired.*

4. Daily Narrative

June 29: Everyone on board by 1430. Transferred from Pier 2 in Kodiak to the fuel dock at USCG at 1720.

June 30: Departed Kodiak at 0145 and began scouting two of our planned profiles: Lines 1 and 2. Steamed by the entrance to Cook Inlet (at northern end of Line 1) and began trip through Shelikof Strait (along Line 12). We observed a lot of marine mammals, mostly whales throughout this scouting, particularly near Cook Inlet. Several areas of particularly shallow water were noted. Low salinity areas were identified near glaciers.

Figure 4.1*. Views of the Alaska Peninsula from Shelikof Strait*

July 1: Continued scouting along Line 12 until 0500. Very shallow water and rocks identified at eastern end of Line 12 and northern end of Line 2. We will shift northern end of Line 2 to the east. Turned south on Line 2 and scouted shallow ridge between Chirkof and Tugidak Islands. Mapped a 6-km-wide ridge with depths of ~35 m of water. Finished scouting at 12:30. Steamed towards the southern end of Line 3. Stopped along the way in deep water (>5000 m) near the trench to do a rosette test with acoustics for OBS work. This required 5 hours and involved lowering the rosette to several depths between 50 and 4500 m and communicating with acoustics. Very calm weather.

July 2: Transited to southern end of Line 3 and began deploying OBS at 0835. Deployed OBS 301-315.

July 3: Continued deploying OBS along Line 3 OBS, finishing with OBS 321 at 0500. Started deploying gun strings at 0545. Began firing mitigation gun, finished deploying the full array, ramped up guns by 1000. Began shooting MGL1110OBS03 at 1100. One power down for marine mammal between OBS 320 and 321 from 1515-1605. Ramped up guns and resumed full power shooting at 1640.

Figure 4.2 *Mladen, Mark, Ron and Tom deploy OBS*

July 4: Continued shooting MGL1110OBS3. Two brief (<9 min) power downs between OBS 301 and 302 at midnight.

July 5: Finished shooting MGL1110OBS3 at 0346. Retrieved air guns (which required one hour) and transited back to first OBS 301. Began OBS recoveries at 0600 and recovered OBS 301-307. Rise times faster than expected (average of ~48 m/min instead of 45 m/min).

July 6: Recovered OBS 308-320.

July 7: Finished recovering OBS at 0100. Transited to southern end of MGL1110OBS05. Relatively rough weather for part of the day (~8-9 ft seas during part of the transit) forced us to shut down multibeam and bring in magnetometer.

Figure 4.3 *Ernie reaches to recover OBS.*

July 8: Began deploying OBS on Line 5 at 0008. Finished deploying all OBS by ~1900. Began deploying guns and turned on mitigation gun at 1920, but had to stop almost immediately because many marine mammals were close to the vessel. But by 2030, we were able to ramp up guns and start shooting MGL1110OBS05T. Started shooting MGL1110OBS05 at 2200. We powered down for marine mammal near beginning of the line. Ramped up the guns while passing OBS 521 and resumed normal shooting at 2323.

July 9: Continued shooting MGL1110OBS05. Intermittent fog. Maggie accumulated a lot of kelp and then became tangled with gun string 2. Both were recovered at 0315. Gun string 2 redeployed 0330. Magnetometer needs a new tow lead, and left onboard until MCS shooting.

July 10: Continued shooting MGL1110OBS05 and finished at 0837. Retrieved the air gun array and transited back to OBS 501, arriving at 10:40. Recovered OBS 501-505.

July 11: Continued recovering OBS on Line 5. Weather began to turn rougher around 0800, with ~8-9 ft swells, but calmed as we went up onto the shelf. Recovered OBS 506-518.

Figure 4.4*. Boat transfer in Sand Point using work boat.*

July 12: Finished recovering OBS on Line 5 at 0310. Steamed up Popof strait to Sand Point for personnel swap via boat transfer. OBS engineers and an NSF marine mammal observer departed. Columbia undergraduates, Dalhousie postdoc and two science techs joined. Arrived at 0610 and departed at 0937. Steamed back out of Popof strait onto shelf and started deploying streamers at 1145. Started by deploying 2 km from Reel 2, then transferred it to Streamer 1 (to obtain 8-km-long cable). Significant time spent replacing bad sections and modules and removing weight from the streamer (which was last used in Costa Rica).

July 13. Continued deploying starboard streamer. Once streamer deployed to bird 4, discovered problem back near connection between Streamers 1 and 2. Recovered streamer to that section, but replacing modules did not solve the problem. Diagnosed as failed slip ring. Began replacing at ~1515. Continued with streamer deployment. Many further sections and modules replaced to correct communications problems.

Figure 4.5*. Jiyao and Andrew attach bird to streamer.*

July 14: Continued deploying starboard streamer, replacing more sections and modules. Streamer completely powered up and completely deployed by ~0600. Deployed head floats and starboard paravane. Deployment of port streamer began thereafter at 0730. Started with streamer 4, then transferred to Streamer 3. Changed some modules and sections near join between two streamers because of telemetry and power issues, but there were only a few other changes thereafter. Finished deployment of port streamer and deployed the port paravane at 2330.

July 15: Shortly after full deployment of the streamers, there was a ground fault in the port streamer. Recovered it from paravane at 0030 to troubleshoot, and discovered that the lead-in failed. Reeled in Streamer 3 by 4 km and transferred to reel 4 by 0445, and deployed 4 km of Streamer 4, retrimming the streamer and replacing sections as needed along the way. Headfloat and port paravane were deployed by 1250. Gun deployment began at 1330 with the mitigation gun beginning at 1426 and deployment finished by 1530. Transited to the beginning of MGL1110MCS05 while ramping up and then firing at full volume. Turned onto MGL1110MCS05 at 1800 and attempted to start acquisition, but communication problem occurred between navigation and recording systems. Troubleshooting of acquisition system for ensuing 7 hours (into July 16) while steaming down the line and turning back to steam to the beginning of the line. Continued shooting throughout troubleshooting with many powerdowns for whales and for a fur seal (at 1930). IHA has zero takes for fur seal, so process with NMFS and NSF initiated. Began shooting test line at 2250 while heading north to start of MGL1110MCS05.

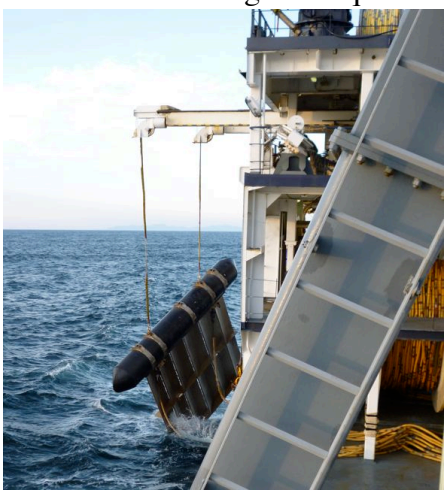

Figure 4.6 *Deploying starboard paravane.*

July 16: Continued shooting test line. Turned onto MGL1110MCS05R and begin acquisition at 0240. Many powerdowns for whales on the line meant that we hardly shot any of the line at full power. Decided to circle back and make one more attempt at shooting. Turned breathlessly close to the coast with all of the gear out one more time, and began acquisition on MGL1110MCS05B at 0722 (sun down local time). Acquisition continued smoothly throughout the day. Began launching XBT and XSV probes every 30 minutes starting at 1840 (water depth of ~300 m) to characterize oceanography from the continental slope to the trench.

July 17: Continued acquisition on MGL1110MCS05B and launching of XBT and XSV every 30 minutes. Powered down for a porpoise at 0100, began ramp up at 0126 and were back at full power by 0146. Continued with XBT's and XSV's until 0452 (water depth of 5650 m). Powered down for a humpback at 1810 and resumed full volume shooting at 1903. Finished MGL1110MCS05B and began MGL1110MCS45 at around 2100.

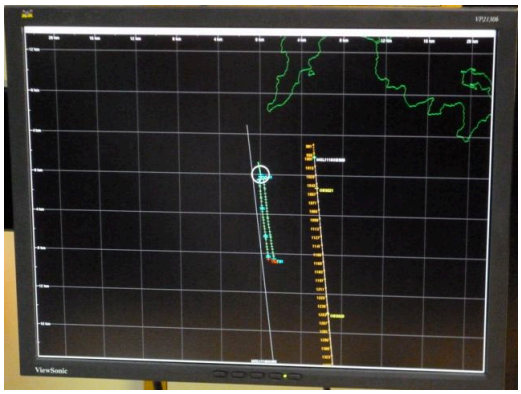

Figure 4.7. *Navigation screen showing close approach to Unga island at northern end of Line 5.*

July 18: Continued acquisition on MGL1110MCS45. One powerdown for marine mammal at 0200. One of guns stopped working at 1120, reducing volume to 6560 cu in. Finished MGL1110MCS45 at 1430 and performed gun maintenance and brief multibeam maintenance while making an outside turn onto MGL1110MCS04. MGL1110MCS04 began at 1733.

July 19: Continued shooting on MGL1110MCS04. At 0230, air gun/spectra problem meant that we did not record 35 shots over Pacific oceanic crust. Started acquiring XBT's and XSV's at 1040 (water depth of ~5000 m). At 1430, recovered PAM, Maggie and portside gun strings. XBT wires became wrapped around PAM which then became tangled in gun strings. Shot with half a source for ~9 km until portside guns were redeployed at 1530. A 7-min-long shot gap occurred again at 1830 due to acquisition system problem. Continued with XBTs until 1928 (water depth of 340 m).

Figure 4.8 *Work boat returning from recovering exploded SRD.*

July 20: Continued shooting on MGL1110MCS04. At 0837, Streamer 1 stopped recording. We decided to finish shooting MGL1110MCS04 recording only on Streamer 2, and attempt to fix Streamer 1 during tie line between MGL1110MCS04 and MGL1110MCS03. Following completion of the line around 1050, the ship experienced engine problems (likely due to kelp in the intake). Starboard engine went offline and other systems were under serious stress and close to failure. Ship speed slowed to <1 kt/h and streamers sank, causing one SRD to go off on Streamer 1. Gun strings retrieved. Starboard engine back online at 1150. Meanwhile, recovered starboard door, head float and lead-in for Streamer 1 to diagnose problems. Several recovery ropes broke on starboard door. Began troubleshot Streamer 1 by by-passing lead-in and/or slip ring. This ultimately revealed that lead-in is close to failure but still working and that slip ring failed. Decided to tow Streamer 1 off the stern (rather than the door). FRC launched at ~1615 to replace SRD on Streamer 1, which was completed by 1750. Afterwards fixed tow point on Streamer 1, and deployed with bypass of slip ring (which will be replaced while we are underway shooting and reconnected between lines). Deployment and ramp up of gun strings began at 2030. Beginning of line MGL1110MCS34 at 2345.

July 21: Finished shooting MGL1110MCS34 at 0300 and turned to MGL1110MCS03T, the transition to the northern end of Line 3. Ended line MGL1110MCS03T and started MGL1110MCS03 at 0700 following turn at entrance to Chignik Bay that brought port door within 2 miles of Castle Rocks. Continued shooting MGL1110MCS03 throughout the day. Multibeam failed a BIST test, mostly likely because of increased ship noise from engines running at high speed, which is not necessary when only one paravane is deployed.

July 22. Continued shooting MGL1110MCS03. Switched over engines to low speed (600 RPMs) because only towing one paravane. This will reduce ship noise (which is particularly detrimental to the bathymetry data). Multibeam then passed BIST test. Began with more XBT and XSV launches at 0210 (water depth of 330 m). Weather worsened as we left the shelf, and began to experience ~12 ft seas. Several shots missed due to crash of Syntrak at 0630. XBT/XSV continued until 1023 (depth of 4013 m). Started to lose data on Streamer 1 at 1230, possibly due to stress on lead-in from rough seas, but it returned at 2045 following reconfiguring after Syntrak crash.

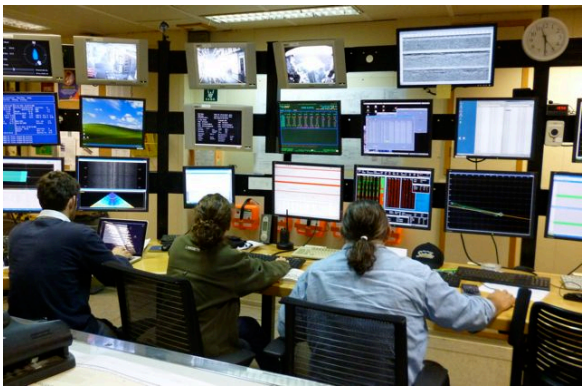

Figure 4.9. *Andrew, Hannah and Mike keep watch.*

July 23: Completed MGL1110MCS03 at 0232. Acquired MGL1110MCS23A from 0338 to 1314. Began MGL1110MCS23B at 1345. Three species of whales were observed from 1550 to 1845, requiring powerdowns and a shut down. Notably, these included a rare sighting of a North Pacific Right whale, which was documented and sent to NMFS. We decided not to attempt to reshoot this part of the line and recommenced shooting at 1945. MGL1110MCS23B completed at 2214, and MGL1110MCS23C started shortly thereafter. Significant swell caused streamer 1 to surface at 2338.

July 24: Continued acquisition of MGL1110MCS23C. Dead beaked whale observed at 0132, which was significant decomposed and thus assumed to have been long dead. PSO's will prepare report for NMFS. Gun string 1 experiencing electrical problems, and attempted to bring in strings 1 and 2 at 0330, but aborted due to significant swells and conditions on the slip way. Postponed until the end of the line. Gun strings became tangled with lead in on Streamer 1 at ~2100 and required 30 min to untangle.

Figure 4.10 *Fluke of humpback whale*

July 25: Finished MGL1110MCS23C at 0045 and pulled in gun strings 1 and 2 for maintenance and repair. Began MGL1110MCS23D at 0523 after maintenance completed. Finished MGL1110MCS23D and began MGL1110MCS02 at ~1120.

July 26: Continued acquisition on MGL1110MCS02. Acquired densely spaced XBT and XSV (<1 km between deployments) on upper part of slope (<2000 m) starting at 0200 and finishing at

0633. Calmer seas on the shelf. Power down for a seal at 0500, but ramped up again by 0538. Powered down for a humpback at 1723. It did not immediately leave the radius, and we were in a critical section of the line near downdip end of locked zone, so circled back to fill in. Ended MGL1110MCS02 at 1800, made turns, and came back on the line at 2200 to start MGL1110MCS02R.

Figure 4.11 *Guns towed behind Langseth*

July 27: Continued acquisition on MGL1110MCS02R. Two more power downs for whales on the shelf at 0312 (returned to full power at 0418) and at 0613 (back at full power at 0622). For the first power down, so many whales were in the area that we decided it would not make sense to circle back. Finished line at 1055, and turned to MGL1110MCS12A. Several power downs required for marine mammals: 1420 for purpoise (back to full power by 1501) and 1550 for whale (back to full power at 1622). Finished MGL1110MCS12A at 1849 (originally named 12M in the acquisition system, but corrected), and began MGL1110MCS1A at 1909. Powered down for whale at 2331. Originally decided to turn around and reshoot, and thus ended MGL1110MCS1A, but then whales cleared out, and we decided to continue and started MGL1110MCS1B at 2349.

July 28: Continued on MGL1110MCS1B. Completed it at 0538, and began MGL1110MCS12B at 0557. Stopped MGL1110MCS12B at 11:48 short of the line end due to tail currents; ship making too fast of speed over ground such that times between shots were shorter than the recording length, and starting skipping shots. Turned onto MGL1110MCS12C and started acquisition again at 1431 with shorter record length (18 s). Made several course adjustments (at 1443, 1544 and 1816) to cross shallow ridge in exact same location as before. Completed MGL1110MCS12C at 2025 and began line MGL1110MCS12D at 2043. Powerdown for mammal at 2343.

Figure 4.12 *Large amounts of kelp accumulated on port paravane lines*

July 29: Continued on MGL1110MCS12D. Ramp up following power down started at 0015 and completed at 0039. Powered down for pair of whales at 0144. Whales continued to be in safety radius for extended period of time (so just firing mitigation gun), and decided to do gun maintenance. Brought in gun strings 1 and 2 for maintenance starting at 0305. Started ramp up with half of the source at 0415. Redeployed strings 1 and 2 at 0435, and had to power down for another mammal shortly thereafter at 0506. Started ramp up near the end of the line. Completed MGL1110MCS12D at 0554, and immediately started MGL1110MCS01C. Ramp up completed shortly thereafter at 0602. Started deploying XBT's, XSV's and XCTD's every ~5 minutes once we came to slope at 1231 and continued until we reached depths of ~2000 m at 1542. At 1748, problems with telemetry on streamer 1 caused acquisition system to crash (not receiving 'end of file'

before next shot), resulting in a loss of ~40 shots while system came back online. The problem recurred repeatedly until 2040 while troubleshooting. Ultimately turned off streamer 1 at 2040 shortly before the line end at 2104, and started recording only on Streamer 2 (although acoustics still working on streamer 1). Pulled in gun strings 3 and 4 for maintenance during and immediately after turn. Started line MGL1110MCS12E at 2124 with half the source. Both gun strings 3 and 4 back in the water and full array firing by 2340.

July 30: Continued on MGL1110MCS12E. Powerdown for porpoise at 0150 and completed ramp up at 0221. Powered down for whale at 0548 and ramped up to full power at 0623. Acquisition system locked up at 1048, missing shots 2838-2843. Completed MGL1110MCS12E at 1244, and relicensed Spectra during turn. MGL1110MCS12F started at 1310. Powered down for whale at 1529 and completed ramp up by 1621.

July 31: Completed MGL1110MCS12F at 0249. Simultaneously powered down for a marine mammal, and back to full power by 0341. Started line MGL1110MCS07 at 0342. Powered down for another mammal at 0714 and ramped up again by 0824. Record length changed back to 22 s from 18 s at 0803 (had been shorter due to tail currents and need to maintain high enough speed through the water for streamer). Record length changed back to 18 s at 1826. Powered down for a mammal at 1949 and back to full power by 2110.

August 1: Continued on MGL1110MCS07. Finished it at 1723, and began line MGL1110MCS56 at 1737.

August 2: Completed MGL1110MCS56 at 0131, shortly after powering down for whales at 0113. Remained powered down or shut down until 0501 (when we returned to full power). Many whales near northern end of lines MGL1110MCS56 and MGL1110MCS06. Some came close enough to the ship that we shut down completely at 0200 before resuming mitigation gun 12 minutes later. Started line MGL1110MCS06 at 0502 following completion of ramp up. Began deploying XBT's at 1305 (water depth of 352 m) and continued until 1340 (depth of 605 m).

August 3: Completed line MGL1110MCS06 at 1211 and began line MGL1110MCS67A at 1239. At 1515, finished line MGL1110MCS67A and began line MGL1110MCS67B at 1530. Completed MGL1110MCS67B at 2258. Ship turned east, and recovery of gun strings commenced at 2330.

Figure 4.13*. The R/V Langseth in port in Dutch Harbor.*

August 4: All gun strings on board by 0020, and recovery of streamer 1 began at 0040. Port door onboard by 0329. Recovery of streamer 4 began at 0400 (both streamers being recovered at the same time). Transferred from Streamer reel 1 to streamer reel 2 at 0620, and from streamer reel 4 to streamer reel 3 at 0642. All gear onboard at 0757 and began transit to Dutch Harbor.

August 5: Continued transit to Dutch Harbor. Turned off ADCP, multibeam and Knudsen at 1357. Meet pilot around 1~430, and were along side by ~1530.

5. Summary of acquisition parameters

Here we briefly summarize the acquisition parameters for the survey. Further detail is given in Appendix B (MCS and OBS specifications)

OBS acquisition

- We used the full 6600 cu in array of the *Langseth* towed at 12 m for all OBS shooting. The array was towed 222.7 m behind the ship's navigational reference point (NRP).
- The shot interval was 310 m (~120 s) for all OBS shooting
- Four-component OBS from Scripps ("LC4x4") recorded continuously during ~3 day deployments at a sampling rate of 5 ms. The sensors used in these OBS are a L28 gimbaled 3-component geophone, and a hydrophone.
- OBS were deployed at spacings of ~15.8 km on Line 3 and ~12.75 km on Line 5.

MCS acquisition

- We used the full 6600 cu in array of the *Langseth* towed at 12 m for all MCS shooting. The array was towed 222.7 m behind the ship's navigational reference point (NRP).
- The shot interval was 62.5 m for all MCS shooting
- A sampling interval of 2 ms was used for all MCS shooting. The record length was 22.528 s on all but two profiles. On parts of both MGL1110MCS07 and MGL1110MCS012C, record lengths were shortened to 18.430 s because of surface currents. The ship needs to maintain a minimum speed through the water when towing the streamers; when tail currents are present, the speed over the ground can be too fast such that the time between shots is too short for the specified record length.
- Several different streamer configurations were used throughout MGL1110, each of which are described below
    - July 15 – July 20 (MGL1110MCS05, 45, 04): Two 8-km-long streamers were used to acquire data. The starboard streamer (Streamer 1) was towed at 9 m and the port streamer (Streamer 2) was towed at 12 m. Streamers were towed from paravanes with nominal separation of 450 m. The distance from the center of the source to the nearest groups on each streamer (channels 636 and 1272, respectively) was 325.84 m.
    - July 20 – July 29 (MGL1110MCS034, 03, 23A, 23B, 23C, 23D, 02, 02R, 12A, 12B, 12C, 12D): Two 8-km-long streamers were used to acquire data. The starboard streamer (Streamer 1) was towed at 9 m and the port streamer (Streamer 2) was towed at 12 m. The port streamer was towed off of a paravane, while the starboard streamer was towed off the stern, resulting in a nominal streamer separation of 225 m. The distance from the center of the source to the nearest groups on the port streamer was 325.84 m and on the starboard streamer was 235.68 m.
    - July 29 – August 3 (MGL1110MCS12E, 12F, 07, 56, 06, 67A, 67B). One 8-km-long streamer (Streamer 2) towed off the port paravane at a depth of 12 m was used to acquire data. The starboard streamer was in the water (in same configuration as above) and provided navigational information, but did not record data. The distance from the center of the source to the nearest groups (channel 636) was 325.84 m.

6. Summary of onboard processing

During MGL1110, we undertook a range on onboard processing activities that are briefly described here and are presented in detail in the appendices.

OBS data (*Appendix C*): We examined both receiver gathers (segy files) and continuous data (miniseed files) from all instruments to check for any problems (e.g., timing errors, mistakes in headers, etc) and to assess data quality. Plots of receiver gathers were generated for all channels on all instruments. We also created spectrograms for all instruments, which illustrate the presence of intermittent 6 Hz noise on some stations as well as increased noise in shallow waters on the shelf. Finally, we picked water wave arrivals and relocated the instruments using a least squares grid search assuming constant water velocity and water depth. A new set of segy files with updated receiver positions and source-receiver offsets were created.

MCS data (*Appendix D*): Brute stacks were generated for all lines using Sioseis on one of the *Langseth*'s workstations (proc1). Sioseis allows the user to vary the velocity function to be used for NMO with water depth. RMS velocity functions were based on a velocity model produced from wide-angle reflection refraction data near Unimak pass (Lizarralde et al., 2002) from the 1994 experiment.

We used Paradigm's Echos to check all of the navigation files (P-190s) and merge them with the raw SEG-D files. The most common problems in the navigation files were near the beginnings and ends, where turns created complications for the acoustic net, and David Martinson reconstructed the streamer location using just the compasses and the GPS. The merged files were written out as Echos DSK files, which can be more readily used for post-cruise processing. Note: At the time of the cruise, Echos only runs properly in the KDE environment.

Multibeam bathymetry data (*Appendix E*): We used MB-system (Caress and Chayes, 2006) on one of the *Langseth*'s workstations (proc2) to perform both automatic data cleaning of spikes and excessive slopes and manual ping editing. Relatively conservative parameters were chosen for automatic cleaning to avoid deleting real arrivals. We focused manual editing efforts on the deep portions of the main MCS dip profiles, where we anticipated interesting targets for imaging, including deformation in the accretionary prism and bending of the downgoing plate. Note: At the time of the cruise, mbsystem only ran properly on the Redhat environment.

Oceanographic data (*Appendix G*) ???? XBT's? looking for reflections in MCS? (put that above?)

7. Initial Results

The high quality of the OBS and MCS data acquired during MGL1110 and our onboard processing efforts (see Section 6) enabled us to observe a remarkable spectrum of exciting features in our new data during the cruise. Below, we briefly summarize some of the exciting preliminary findings based on OBS and MCS data.

Deep reflections off the megathrust and other faults in the overriding plate

Shipboard brute stacks of MCS data from all of the dip profiles and some strike profiles reveal reflections over the length of the megathrust, including it's updip extent near the trench, the locked region, and the estimated downdip transition to stable sliding. We also observe prominent reflections within the overriding plate (e.g., Fig 7.1).

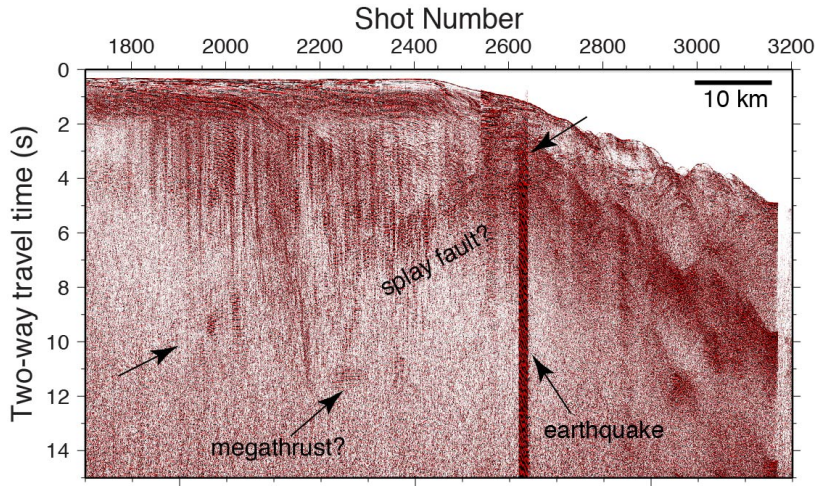

Figure 7.1. *Brute stack on landward portion of MGL1110MCS05 showing reflections that are interpreted to originate within the crust and from the megathrust.*

Just landward of the trench, one or more bands of reflections appear to be associated with the subducting plate, which may arise from subducting sediments, the top of oceanic crust and/or the oceanic Moho. Farther seaward in the portion of the megathrust thought to be locked based on geodetic data, the character of reflections interpreted to originate from megathrust is highly variable along and across strike. Bright reflections over limited distances are observed in some places while other areas are characterized by weak or absent megathrust reflectivity. Farther downdip, high amplitude bands of reflections are common on the portions of the megathrust near the downdip edge of the locked zone and transition to stable sliding based on geodetic data (Fig. 7.2). Initial inspection indicates that these bands appear to be as wide as ~2 s two-way travel time (twtt) in brute stacks, and are commonly observed to at least 14-17 s twtt on all dip profiles. We also observe bright wide-angle reflections at source-receiver offsets of ~60-120 km in OBS receiver gathers (Fig. 7.3)

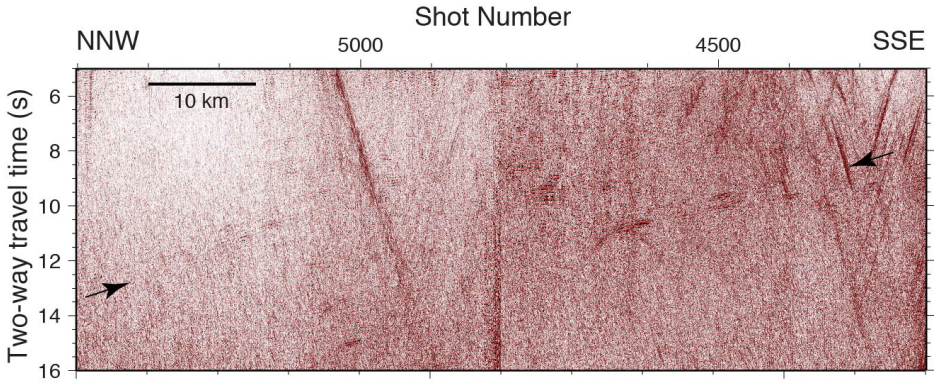

Figure 7.2*. Example of deep bright reflections interpreted to arise from the megathrust on Lines MGL1110MCS02 and 02R (joined at shot 4800).*

Many other bright reflections are observed within the overriding plate. Some of the most continuous and bright intracrustal reflections in brute stacks appear to delineate one or more large splay faults (Fig. 7.1). On some profiles, these

splay faults are clearly associated with basins with fanning sediments, possibly imply large amounts of cumulative deformation over long periods of time (Fig. 7.1). Many of these features can be observed to connect to the interpreted megathrust in brute stacks. Their location with respect to the continental shelf changes (some are within the shelf, others at the edge).

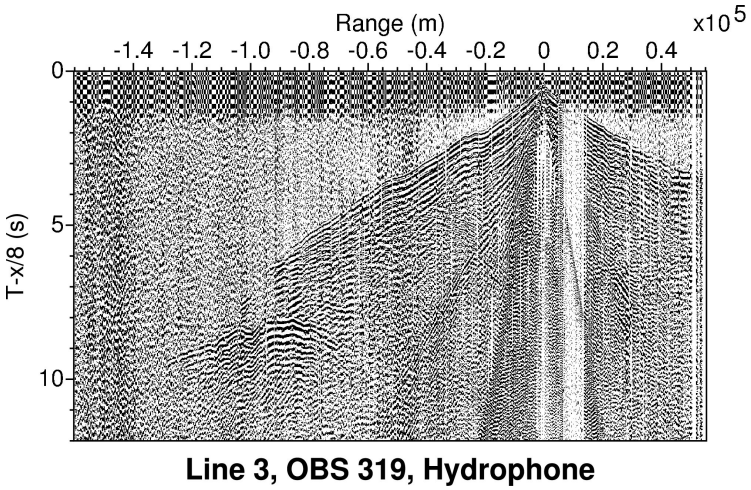

Figure 7.3 *Receiver gather from OBS 319 (near landward end of Line 3 OBS). Note bright reflections at offsets of 60-120 km that we tentatively interpret as arising from the megathrust.*

Bending and hydration of the downgoing plate

Farther seaward, reflection data reveal remarkable variations in the structure of the downgoing plate from one profile to another. Abundant normal faulting is observed on the western dip profiles MGL1110MCS04, 05 and 06, where the plate is subducting in the weakly coupled Shumagin Gap (Fig. 7.4). Brute stacks from MGL1110MCS04 and 05 reveal clear faulting of the sediments and upper oceanic crust with fault offsets of ~0.1-0.2 s twtt (Fig. 7.4). Bending-related faulting is also apparent in multibeam bathymetry data (Fig. 7.5). Less bending-related deformation appears to be associated with MGL1110MCS03, which images the subducting plate in the center of the Semidi segment. Basement topography (possibly associated with deformation of the basement) is observed on this profile, but the overlying sediments usually appear to drape this topography suggesting it was not active during bending (and instead created by spreading processes). At the eastern end of the Semidi segment on MGL1110MCS02, high-amplitude basement topography is apparent (0.5-1.0 s twtt), possibly associated with seamounts that are also observed in multibeam bathymetry data; it is unclear to what extent this basement has been deformed during bending.

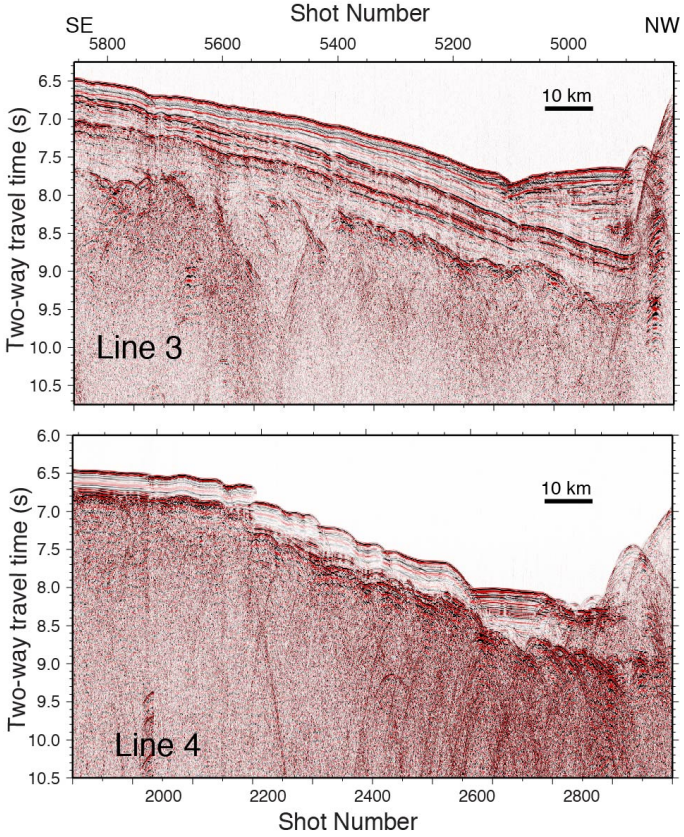

Figure 7.4 *Comparison of bending-related faulting on brute stacks of MGL1110MCS03 and 04.*

The profiles also vary in the distribution and thickness of sediments. Sediments overlying oceanic basement on MGL1110MCS04, 05 and 06 reach a maximum thickness of 0.5 s twtt, while on MGL1110MCS03, sediment thicknesses exceed 1 s twtt. Very little sediment locally overlies basement on MGL1110MCS02 owing to the rugged topography sampled by this line.

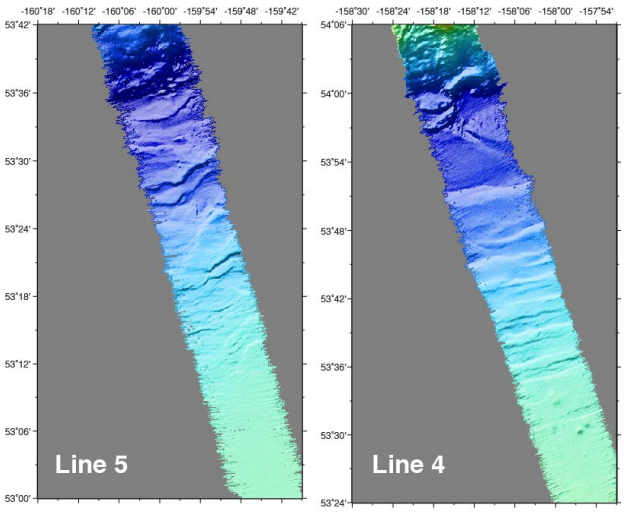

Figure 7.5 *Multibeam bathymetry data over seaward ends of MGL1110MCS04 and 05 in areas where significant bending related faulting is apparent in MCS data. The trench is the deepest area (dark blue) on both profiles. Farther south, features with orientations parallel to the trench (WSW-ENE) and parallel to the fabric of incoming oceanic crust (E-W) are apparent, particularly on Line 5.*

Finally, other aspects of the crustal structure appear to vary between profiles in Shumagin Gap and the Semidi segment. MGL1110MCS05 exhibits a bright, continuous oceanic Moho reflection in both MCS and OBS data (e.g., Fig. 7.6). Moho is weak to absent on MGL1110MCS03. There also appear to be changes in the velocity structure of the downgoing plate based on initial inspection of wide-angle data; for example, there are large changes in moho reflectivity (Fig. 7.6). These velocity patterns could be explained by variable hydration.

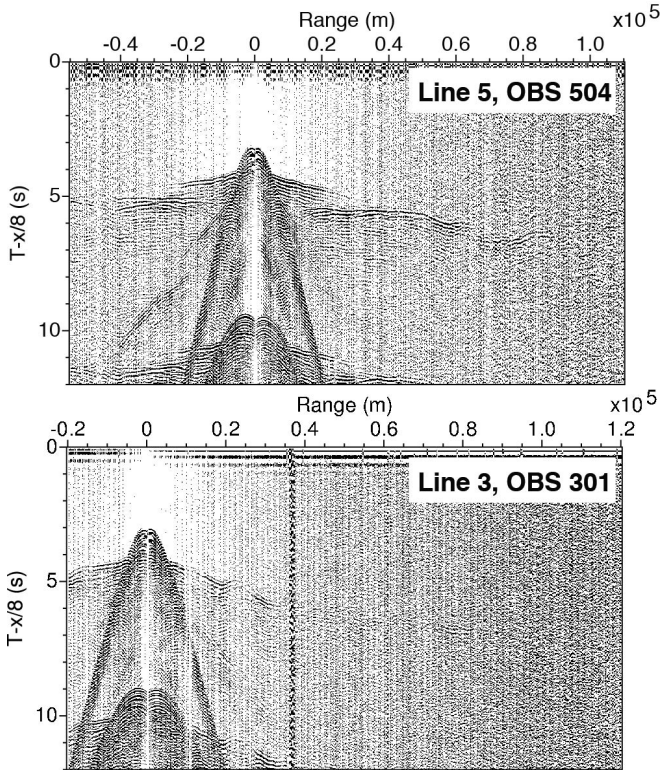

Figure 7.6 *Comparison of OBS data from Line 5 in the Shumagin gap and Line 3 in the Semidi segment showing variations in Moho reflectivity and apparent velocities of crust and mantle. Also note the apparent low velocity zone near base of crust on Line 5.*

There are a number of possible explanations for preliminary observations of along-strike variability of the downgoing plate. One is the orientation of pre-existing fabrics in the downgoing oceanic crust. Due to complexities in the spreading history of subducting Pacific crust associated with Kula and Farallon plates (e.g., Lonsdale, 1988), there is nearly a 90º change in the spreading direction that emplaced downgoing oceanic crust with respect to the trench between the Shumagins and the Semidi segments. The spreading direction (and presumably faults created by spreading processes) parallel the trench in the Shumagin Gap and are perpendicular to the trench in the Semidi segment (as illustrated by maps of magnetic anomalies, Fig. 7.7). Crust with favorably oriented pre-existing faults might be more readily deformed and serpentinized during

bending south of the trench. The dip of the subducting oceanic plate also increases to the southwest, which may account for enhanced bending-related deformation here. Our data also reveal other apparent variations in the structure of the downgoing plate, such as variations in thickness, moho reflectivity, sills in the crust and mantle, etc. Some of these variations may be associated with a failed triple junction (see next section) that may also influence subduction processes. More work is required to characterize variations in the structure of the downgoing plate and differentiate between possible contributing factors. But the combined preliminary observations of variations in the structure of the downgoing plate between areas with different coupling described above may imply an important role for the properties of the downgoing plate in slip behavior and seismogenesis at subduction zones.

Imaging of failed triple junction

Serendipitously, we also acquired data over a fossil ridge-ridge-ridge triple junction that once separated the Pacific, Kula and Farallon plates. Reflections are captured from depths as great as some ~15 km into the lithosphere surrounding this fossil triple junction. These reflections could possibly be caused by gabbroic melts that were once percolating upward but froze in the crust and mantle lithosphere when the triple junction was abandoned during a plate reorganization in Early Tertiary. We plan to use our reflection data to characterize crustal and upper mantle structure around this feature and extract new insight into the deep structure of triple junctions, how they operate, and what happens when they fail.

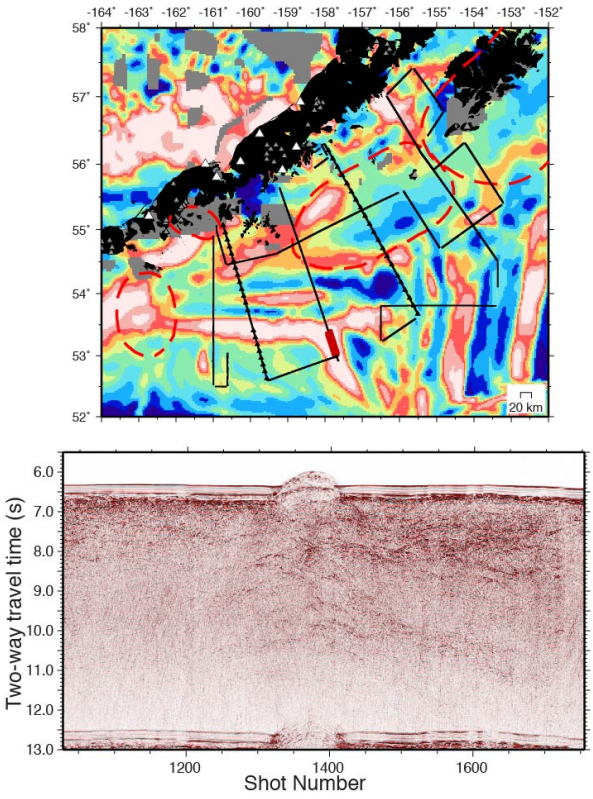

Figure 7.8 *Above: Magnetic anomalies overlain by locations of profiles (black lines), OBS (black triangles) and temporary onshore stations (white triangles) and existing seismometer locations (grey triangles). Triple junction is manifest by T-shaped magnetic high centered at 53.25ºN, 158ºW. Red line: location of MCS profile below. Below: Brute stack from MGL1110MCS04 crossing the fossil triple juction.*

Shallow fine scale structure in the water column

XBT/XSV data acquired throughout the cruise and initial processing of MCS data also provide some early insights in ocean structure. Oceanographic data show a warm temperature layer below the mixing layer and above 400 m depth that was attached to the continental slope. An example of single profile acquired in the survey is shown in Figure 7.9, which shows some fine structure above 400 m depth and smooth profiles at deeper water. The seismic data that were processed on board show very weak reflections above 400 m depth, strongly affected by the direct wave. Better processing must be done in order to remove the direct wave and to enhance the weak reflectivity of the water to better illuminate ocean structure.

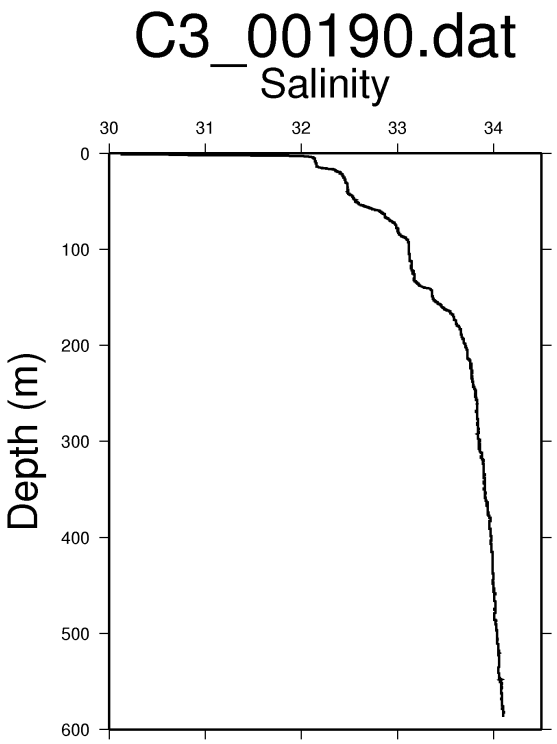

***Figure 7.9**: Example of salinity profile acquired on Line 1C using an XCTD.*

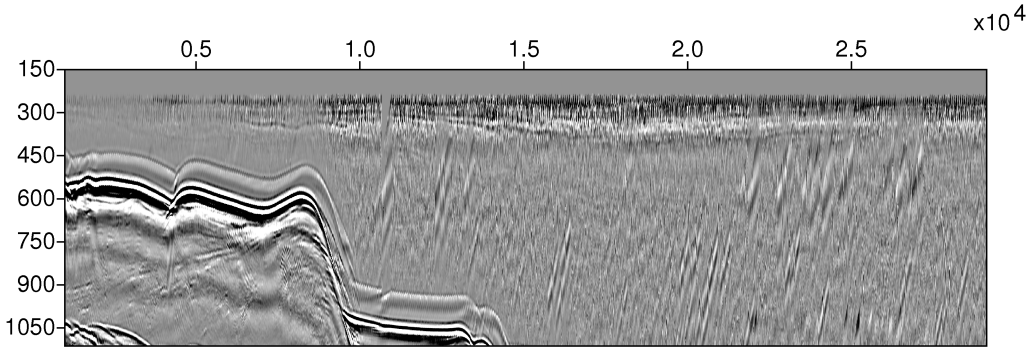

***Figure 7.10**: Stacked seismic section of Line 1C.*

8. Performance of the *Langseth*

Overall, we found the *Langseth* to be in great condition, and the technical staff and crew are excellent. Below we summarize our experience with different aspects of operations and facilities.

MCS equipment

The *Langseth* has vastly superior seismic capabilities to any other academic vessel in the world. The data that we were able to acquire using the large, tuned air-gun array and multiple 8-km-long streamers are tremendous and essential for addressing our scientific objectives. However, all of this equipment is relatively old and aging. A disproportionate number of components failed during our program, including many streamer sections and modules, two lead-in's and two slip rings. Spares were available to replace modules and streamer sections, but fixing these issues required a considerable amount of time and brawn on the part of the technical staff and science party. Likewise, spare slip rings were also available, but required some downtime to replace. However, there were no spare lead-in's except for those on the streamer reels that were not being used. We were able to address the failure of the lead-in on Reel 3 by shifting the port streamer from Reel 3 to Reel 4, which required the time to bring in part of one streamer, move it to Reel 4, and deploy streamer from the new reel, and retrim and replace of sections on this part of the streamer. However, the failure of the second lead-in meant that we were only able to acquire data on one streamer for the later part of the program. We understand that the *Langseth* does not currently possess spares for lead-in's. To the extent that it is possible, we recommend that the *Langseth* acquire and carry spares for lead-in's and other components of streamers in addition to spare sections and modules. We also suggest that an annual maintenance cruise (akin to MGL1104 off San Diego in March 2011) would allow more assessment and maintenance of the MCS equipment.

The acquisition system is relatively clunky – problems with it caused to a significant amount of downtime at the beginning of MCS acquisition (~7 hours), and it crashed several times during operations, leading to lost data. It is not clear that there is an immediate solution to this problem, other than the acquisition of new streamer (which is an expensive prospect).

Lab facilities and onboard computing

Overall, the computational facilities on the *Langseth* are excellent and met our purposes. The *Langseth* possesses two fast workstations and ample disk space that can be used by the science party for onboard processing. We only experienced a few minor obstacles, which are described below.

Based on the information received before the cruise, we decided to use these workstations (plus our Mac laptops) for our onboard processing rather than bring our own workstations. We were able to use the *Langseth's* machines to complete a range of important onboard processing jobs, including merging navigation and seg-d file, generating brute stacks and editing bathymetry data. A number of processing packages are nominally installed on these stations, but some time was required at the beginning of the cruise to get them working. Echos (focus) worked very well for us during MGL1110 (following trouble shooting that was apparently done during MGL1109). However, neither sioseis nor MB-system were operational when we arrived on this ship, so this required a little bit of time and effort to solve (with the help of Paul Henkart). We reinstalled

Sioseis, and discovered that MB-system only worked in the Gnome environment after some trouble shooting. Based on information received before the cruise from the Marine Office, we expected all of these (relatively) standard packages to be installed and fully functional. However, the technical staff on the ship do not have time to maintain these machines and/or install and troubleshoot any software/programs that the science party might want to use. This needs to be clearly communicated to the science party before the cruise so that they can prepare accordingly.

Although nearly every cruise aboard the *Langseth* must involve copying a large volume of seismic data from the *Langseth's* system to portable disks, there was not a well-developed system for doing this. We had to try many approaches to copy the ~6 Tb of raw and shipboard processed data generated during MGL1110 to the USB disks brought by the science party, so that a couple of days were needed to arrive at an effective system. Some USB ports and network connections were too slow to complete the copy job by the end of the cruise, even though we started early. We recommend that one or more 'standard' procedures be developed for copying data and that more advice could be supplied to the science party before the cruise. For example, some of the technical staff told us that using networked drives rather than USB drives would facilitate copying data (although these might be more complicated and time intensive to mount and set up). Another solution is that the science party could bring a laptop dedicated to data backup that permitted writing/reading disks for any file system. Alternatively, there could be a machine on the *Langseth* with good USB connectivity that permitted writing disks for any file system. If there is a particular type of media that should be brought to efficiently copy data, which should be clearly communicated to the science party before the cruise.

Technical staff

The technical staff aboard MGL1110 are uniformly dedicated and capable, and did an excellent job in the challenging circumstances of our cruise. Robert Steinhaus and David Martinson, in particular, are the heart of the operation. They know the ship's systems inside and out, and worked brutally long hours to make the cruise a success. Their excellence highlights a weakness: there does not appear to be anyone else who possesses comparable experience or knowledge of the entire operation who can fill their roles, so the entire operation is really dependent on them. We recommend training of current staff or hiring of new staff to begin to address this issue if it is not being done already. The other permanent staff were also extremely good - familiar with many aspects of the ship's systems and capable of solving problems that arose. Although the contractors were good and dedicated, they were naturally much less familiar with many of the ship's systems and less able to solve problems that arose during the cruise. We recommend that the *Langseth* would opt for hiring permanent employees over using contractors to the extent that this is possible. The *Langseth* is an extremely complicated platform, so its not possible for new people to operate at anything close to the same level as trained, experienced permanent employees.

Living conditions

The accommodation spaces, galley and other leisure spaces (movie room) were in excellent shape. Those in our science party who had participated on previous *Langseth* cruises prior to the most recent renovations were especially impressed by the improvements. The gym was in excellent shape and in a nice location. The cooks did an excellent job of preparing varied food in

an attempt to satisfy everyone's desires, but we would still request more healthy food, particularly at lunch (where a large portion of food was fried). Stocking more whole wheat bread and healthy snacks would also be great. Over the course of the cruise, many of the healthier food options were quickly depleted (yogurts, V8's, etc). As the ship's staff are already aware, Hi-Seas net is very slow and did not seem very reliable. It regularly crashed for short periods of time (requiring multiple reboots per day), and we had about 2 days total during which we had not internet connectivity. We recommend that other options be explored.

9. References

Audet, P., M. G. Bostock, N. I. Christensen, and S. M. Peacock (2009), Seismic evidence for overpressured subducted oceanic crust and megathrust fault sealing, Nature, 457, 76-78, doi:10.1038/nature07650.

Brown, J. R., S. G. Prejean, G. C. Beroza, J. S. Gomberg, and P. J. Haeussler (2010), Evidence for Deep Tectonic Tremor in the Alaska-Aleutian Subduction Zone, EOS Trans AGU, Fall Meet. Suppl., S23A-2091.

Caress, D. W., and D. N. Chayes, MB-System: Mapping the Seafloor, http://www.mbari.org/data/mbsystem and http://www.ldeo.columbia.edu/res/pi/MB-System, 2006.

Cloos, M., (1992). Thrust-type subduction-zone earthquakes and seamount asperities -- a physical model for seismic rupture. Geology 20, 601-604.

Cummis, P.F; Cherniawsky, J. Y. And Foreman, M. G. G. 2001. North Pacific internal tides from the Aleutian Ridge Altimeter observations and modeling. Journal of Marine Research, 59, 167-191.

Davies, J., L. Sykes, L. House, and K. Jacob (1981), Shumagin Seismic Gap, Alaska Penninsula: History of Great Earthquakes, Tectonic Setting, and Evidence for High Seismic Potential, J. Geophys. Res., 86, 3821-3855.

Fisher, M. A., T. M. Brocher, W. J. Nokleberg, G. Plafker, and G. L. Smith (1989), Seismic reflection images of the crust of the northern part of the Chugach Terrane, Alaska: Results of a survey for the Trans- Alaska Crustal Transect (TACT), J. Geophys. Res, 94, 4424-4440.

Fournier, M., P. Huchon, K. Khanbari, and S. Leroy (2007), Segmentation and along-strike asymmetry of the passive margin in Socotra, eastern Gulf of Aden: Are they controlled by detachment faults?, Geochem. Geophys. Geosys., 8, Q03007, doi:03010.01029/02006GC001526.

Fournier, T. J., and J. T. Freymueller (2007), Transition from locked to creeping subduction in the Shumagin region, Alaska, Geophys. Res. Lett., 34, L06303, doi: 06310.01029/02006GL029073.

Freymueller, J., and J. Beavan (1999), Absence of Strain Accumulation in the Western Shumagin Segment of the Alaska Subduction Zone, Geophys. Res. Lett., 26(21), 3233-3236.

Groß, K., U. Micksch, and TIPTEQ Research Group Seismic Team (2008), The reflection seismic survey of project TIPTEQ - the inventory of the Chilean subduction zone at 38.2ºS, Geophys. J. Int., 172, 565-571.

Holbrook, W. S., P. Páramo, S. Pearse, and R. W. Schmitt (2003), Thermohaline fine structure in an oceanographic front from seismic reflection profiling, Science, 301, 821–824, doi:10.1126/science.1085116.

Hyndman, R.D., Wang, K., 1993. Thermal constraints on the zone of major thrust earthquake failure: the Cascadia subduction zone. J. Geophys. Res. 98, 2039–2060.

Hyndman, R. D., and K. Wang (1995), The rupture zone of Cascadia great earthquakes from current deformation and the thermal regime, J. Geophys. Res., 100(B11), 22133-22154.

Ivandic, M., I. Grevemeyer, A. Berhorst, E. R. Flueh, and K. McIntosh (2008), Impact of bending related faulting on the seismic properties of the incoming oceanic plate offshore of Nicaragua, J. Geophys. Res., 113, B05410, doi:05410.01029/02007JB005291.

Kodaira, S., E. Kurashimo, J.-O. Park, N. Takahashi, A. Nakanishi, S. Miura, T. Iwasaki, N. Hirata, K. Ito, and Y. Kaneda (2002), Structural factors controlling the rupture process of a

megathrust earthquake at the Nankai trough seismogenic zone, Geophys. J. Int., 149, 815-835.

Kodaira, S., T. Iidaka, A. Kato, J.-O. Park, T. Iwasaki, and Y. Kaneda (2004), High Pore Fluid Pressure May Cause Silent Slip in the Nankai Trough, Science, 304, 1295-1298.

Ladd, C.; Stabeno. P. And Cokelet, E.D. 2005. A note on cross-shelf exchange in the northern Gulf of Alaska. Deep-Sea Research II, 52, 667-679.

Lizarralde, D., W. S. Holbrook, S. McGeary, N. Bangs, and J. Diebold (2002), Crustal construction of a volcanic arc, wide-angle seismic results from the western Alaska Peninsula, J. Geophys. Res., 107(8), 21.

McCaffrey, R. (2007), The Next Great Earthquake, Science, 315, 1675-1676.

Mirshak, R., Nedimović, M.R., Greenan, B. J. W., Ruddick, B. R., Louden, K.E., (2010) Coincident reflection images of the Gulf Stream from seismic and hydrographic data Geophys. Res. Lett., 37, L05602, doi:10.1029/2009GL042359.

Moore, J. C., J. Diebold, M. A. Fisher, J. Sample, T. Brocher, M. Talwani, J. Ewing, R. von Huene, C. Rowe, D. Stone, C. Stevens, and D. S. Sawyer (1991), EGDE deep seismic reflection transect of the eastern Aleutian arc-trench layered lower crust reveals underplating and continental growth, Geology, 19, 420-424.

Müntener, O., P. B. Kelemen, and T. L. Grove (2001), The role of H2O during crystallization of primitive arc magmas under uppermost mantle conditions and genesis of igneous pyroxenites: an experimental study, Contributions to Mineralogy and Petrology, 141, 643-658.

Nedimović, M. R., R. D. Hyndman, K. Ramachandran, and G. D. Spence (2003), Reflection signatures of seismic and aseismic slip on the northern Cascadia subduction interface, Nature, 424, 416-420.

Nedimović, M. R., Mazzotti, S. and Hyndman, R. D., 3D structure from feathered 2D seismic reection data; The eastern Nankai trough, J. Geophys. Res. 108, 1-14, 2003.

Nedimović, M. R., Bohnenstiehl, D. R., Carbotte, S. M., Canales, J. P. and Dziak, R. P., Faulting and hydration of the Juan de Fuca plate system, Earth Planet. Sci. Lett. 284, 94-102, 2009.

Oleskevich, D. A., R. D. Hyndman, and K. Wang (1999), The updip and downdip limits to great subduction earthquakes: Thermal and structural models of Cascadia, south Alaska, SW Japan, and Chile, J. Geophys. Res., 104, 14965-14991.

Petersen, C. J., and D. H. Christensen (2009), Possible relationship between nonvolcanic tremor and the 1998–2001 slow slip event, south central Alaska, J. Geophys. Res, 114, doi:10.1029/2008JB006096.

Peacock, S.M., and R.D. Hyndman, (1999). Hydrous minerals in the mantle wedge and the maximum depth of subduction thrust earthquakes. Geophys. Res. Lett. *26*, 2517-2520.

Ranero, C. R., J. Phipps Morgan, K. McIntosh, and C. Reichert (2003), Bending-related faulting and mantle serpentinization at the Middle America trench, Nature, 425, 367-373.

Ruff, L., and H. Kanamori, (1980). Seismicity and the subduction process. Phys. Earth and Planet. Int. 23, 240-252.

Ruff, L. J., and H. Kanamori (1983), Seismic coupling and uncoupling at subduction zones, Tectonophys., 99, 99-117.

Ruff, L. J. (1989), Do Trench Sediments Affect Great Earthquake Occurrence in Subduction Zones?, Pageoph, 129, 263-282.

Scholz, C.H., (1998). Earthquakes and friction laws. Nature 391, 37-42.

Sykes, L. R., J. B. Kisslinger, L. House, J. N. Davies, and K. H. Jacob (1971), Rupture zones and repeat times of great earthquakes along the Alaska-Aleutian arc, 1784-1980, Maurice Ewing Series, 4, 73-80.

Tichelaar, B.W., and L.J. Ruff, (1993). Depth of seismic coupling along subduction zones. J. Geophy. Res. 98, 2017-2037.

Uyeda, S., and H. Kanamori, (1979). Back-arc opening and the mode of subduction. J. Geophys. Res. 84, 1049-1061.

Wada, I., and K. Wang (2009), Common depth of slab-mantle decoupling: Reconciling diversity and uniformity of subduction zones, Geochem. Geophys. Geosys., 10(10), Q10009, doi:10010.11029/12009GC002570.

Zweck, C., J. T. Freymueller, and S. C. Cohen (2002), Three-dimensional elastic dislocation modeling of the postseismic response to the 1964 Alaska earthquake, J. Geophys. Res., 107, 2064, doi:2010.1029/2001JB000409.

Appendix A: Cruise participants

Scientific and Ship Crew

Ship Crew
James O'Loughlin, Master
Stanley Zeigler, Chief Mate
David Wolford, 2nd Mate
West Wilson, 3rd Mate
Ricardo Redito, Bosun
Matthew Ursin, AB
George Cereno, AB
Inocencio Rimando, AB
Jeromiel Webster, OS
Nicky Applewhite, OS
Albert Karlyn, Chief Engineer
Ryan Vetting, 2nd Engineer
Trevor Lapham, 3rd Engineer
Clayton Busenga, 3rd Engineer
Philip Neis, Electrician
Rodolfo Florendo, Oiler
Jerald Chase, Oiler
Stephen Graves, Oiler
Hervin McLean Fuller, Steward
Leoncio Martires, Cook

Scientific Party, OBS Leg 1
Donna Shillington, Chief Scientist
Mladen Nedimović, Co-chief Scientist
Spahr Webb, Co-chief Scientist
Anne Bécel, LDEO research scientist
Matthias Deleschluse, ENS professor
Jiyao Li, LDEO PhD student
Harold Kuehn, PhD student
Aaron Farkas, Dalhousie McS student
Ernie Aaron, OBS Engineer
Mark Gibaud, OBS Engineer
Phil Thai, OBS Engineer
Ron Kao, OBS Engineer

Shipboard Technical Staff, OBS Leg 1
Robert Steinhaus, Chief Science Officer
Michael Martello, Navigation/IT

Ryan Eaton, Acquisition Leader
Thomas Spoto, Chief Source
Weston Groves, Source Mechanic
Jamee Johnson, Source Mechanic
Michael Tatro, Source Mechanic
Meagan Cummings, PSO
Kendra Davis, PSO
Olivia Lee, PSO
Stephanie Milne, PSO
Christine Voigtlander, PSO
Meghan Wood, PSO

Scientific Party, MCS Leg 2
Donna Shillington, Chief Scientist
Mladen Nedimović, Co-chief Scientist
Spahr Webb, Co-chief Scientist
Anne Bécel, LDEO research scientist
Matthias Deleschluse, ENS professor
Berta Biescas Gorriz, Dalhousie postdoc
Jiyao Li, LDEO PhD student
Harold Kuehn, PhD student
Aaron Farkas, Dalhousie McS student
Celia Eddy, Columbia undergrad
Kelly Hostetler, Columbia undergrad
Hannah Perls, Columbia undergrad
Andrew Wessbecher, Columbia undergrad
Jack Zietman, Columbia undergrad

Shipboard Technical Staff, MCS Leg 2
Robert Steinhaus, Chief Science Officer
David Martinson, Chief Navigation
Michael Martello, Navigation/IT
Ryan Eaton, Acquisition Leader
Charles (Gram) Erwin, Acquisition Leader
Thomas Spoto, Chief Source
Weston Groves, Source Mechanic
Jamee Johnson, Source Mechanic
Michael Tatro, Source Mechanic
Meagan Cummings, PSO
Kendra Davis, PSO
Stephanie Milne, PSO
Christine Voigtlander, PSO
Meghan Wood, PSO

Scientific Party Contact Information

Donna Shillington
Lamont Doherty Earth Observatory, Columbia University
djs@ldeo.columbia.edu
work: +1 845-365-8818
mobile: +1 646-678-0081

Mladen Nedimovic
Dalhousie University, Lamont Doherty Earth Observatory, Columbia University
mladen@dal.ca
902-494-4524

Spahr Webb
Lamont Doherty Earth Observatory, Columbia University
scw@ldeo.columbia.edu
845-365-8439

Anne Bécel
Collège de France, Aix-en-Provence, France (current)
Lamont Doherty Earth Observatory, Columbia University (after September 1, 2011)
annebcl@gmail.com
+33 760 361240

Berta Biescas
Unitat de Tecnologia Marina CSIC (current)
Dalhousie University (after September 1, 2011)
biescas@cmima.csic.es
34 65033006

Matthias Deleschluse
Laboratoire de Géologle de l'Ecole normale supérieure
delescluse@geologie.ens.fr
+33 01 44322262

Aaron Farkas
Dalhousie University
aaron.farkas@unb.ca
506-471-3643

Harold Kuehn
Dalhousie University
hkuehn82@googlemail.com

Jiyao Li
Lamont Doherty Earth Observatory, Columbia University

jiyao.lee@gmail.com
718-536-4011

Celia Eddy
Lamont Doherty Earth Observatory, Columbia University
celialeddy@gmail.com
917-656-6965

Kelly Hostetler
Lamont Doherty Earth Observatory, Columbia University
Krh2114@columbia.edu
509-521-1857

Hannah Perls
Lamont Doherty Earth Observatory, Columbia University
hnperls@gmail.com
617-733-7894

Andrew Wessbecher
Lamont Doherty Earth Observatory, Columbia University
wessbecher@gmail.com
951-375-9875

Jack Zietman
Lamont Doherty Earth Observatory, Columbia University
jzietman@gmail.com
978-979-4135

Ernie Aaron
Scripps
eaaron@ucsd.edu
858-534-8229

Phil Thai
Scripps
pthai@ucsd.edu

Group photo of MGL1110

*some people who could not be in the original photo have been added digitally

Scientific Watch Schedule

OBS Leg 1

Shipboard Technical Staff
Day watch (12pm-12am)
Ryan Eaton (Watch Leader), Weston Groves, Tom Spoto

Night Watch (12am-12pm)
Mike Martello (Watch Leader), Mike Tatro, Jamee Johnson

OBS Team
Day watch (12pm – 12am)
Matt Gibaud, Phil Thia

Night Watch (12am – 12pm)
Ernie Aaron, Ron Kao

Science party
12am – 6am
Anne Bécel, Matthias Deleschluse
6am – 12pm
Donna Shillington, Jiyao Li
12pm – 6pm
Mladen Nedimović, Harold Kuehn
6pm – 12am
Spahr Webb, Aaron Farkas

MCS Leg 2

Shipboard Technical Staff
Day watch (12pm-12am)
David Martinson, Ryan Eaton, Tom Spoto, Weston Groves

Night Watch (12am-12pm)
Mike Martello, Gram Erwin, Mike Tatro, Jamee Johnson

Science party
12am – 6am
Anne Bécel, Matthias Deleschluse, Jack Zietman
6am – 12pm
Donna Shillington, Jiyao Li, Hannah Perls, Andrew Wessbecher
12pm – 6pm
Mladen Nedimović, Harold Kuehn, Kelly Hostetler, Berta Biescas*
6pm – 12am
Spahr Webb, Aaron Farkas, Celia Eddy